CHAPTER

16 Waveguide circuits

In this chapter we examine rectangular metal waveguides and, in particular, their most common mode of operation, the fundamental "TE_{10}" mode. We will also see how the concepts developed for two-conductor transmission lines apply to waveguides and look at waveguide versions of some low-frequency components.

The ability of a hollow metal pipe to transmit electromagnetic waves can be demonstrated by holding it in front of your eye. You can see through it, so, at least, it passes electromagnetic waves of extremely short wavelengths. From a purely dimensional analysis, you would guess correctly that the longest wavelength a pipe could transmit must be of the order of the pipe's transverse dimensions. It turns out that, for propagation in a rectangular pipe, the free-space wavelength, c/f, must be less than twice the longer transverse dimension and, for a circular pipe, less than 1.706[1] times the diameter. Waveguides have less loss and more power handling capacity than coaxial lines of the same size and they need no center conductor nor insulating structures to support a center conductor. Metal waveguides are used most often in the range from 1000 MHz to 100 GHz, where they have practical dimensions. Waveguides for optical frequencies are coated glass fibers.

16.1 Simple picture of waveguide propagation

A common RF engineering argument for the plausibility of transmitting electromagnetic waves through a hollow metal pipe is shown in Figure 16.1, where a two-conductor transmission line evolves into a waveguide. Quarter-wave shorted stubs are added to the line. Since a shorted quarter-wave line presents an open circuit, these stubs do not short the line. More stubs are added to both sides until a rectangular pipe is formed.

This plausibility argument, while not rigorous, does illustrate some important properties of waveguide propagation in the fundamental mode (the

[1] The factor 1.706 is $\pi/1.841$, where 1.841 is the smallest root of the equation $\mathrm{d}/\mathrm{d}x\, J_1(x)=0$ and $J_1(x)$ is the first-order Bessel function of the first kind, a function whose shape resembles $\sin(x)/(x+1)^{1/2}$.

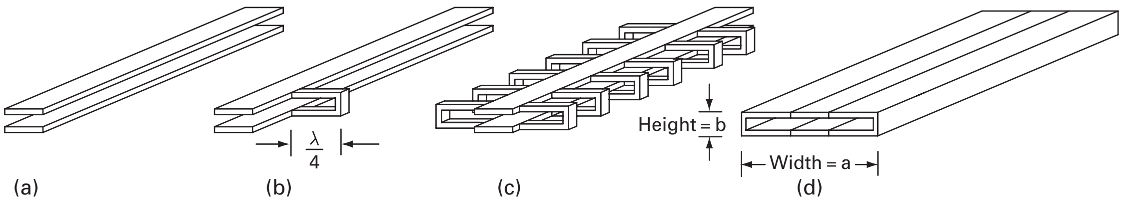

Figure 16.1. Transmission line-to-waveguide evolution. Shorted quarter-wave stubs do not short the transmission line.

simplest and lowest frequency mode): the electric field, which is essentially vertical between the conductors in Figure 16.1(a), becomes perfectly vertical in the waveguide, though its magnitude must fall to zero at the waveguide's sides, since the metallic walls short out any tangential electric field. And, just as the conductors of the transmission line of Figure 16.1(a) can have any separation and still support wave propagation, the waveguide of Figure 16.1(d) can have any height. The width, however, is critical. The total width of the guide must be at least $\lambda/2$ to accommodate a quarter-wave stub on each side and still have nonvanishing conductor strips, as shown in Figure 16.1(c). This means that there is a low-frequency cutoff; wave propagation is not possible if the wavelength is greater than $2a$ where a is the waveguide width (the longer dimension).

Standard waveguide designations indicate the shape and size of the guide. WR430, for example, denotes "Waveguide, Rectangular," 4.3 inches (10.9 cm) wide. The standard width-to-height ratio is two-to-one. (While the height of the guide can be made arbitrarily small, the waveguide will become increasingly lossy because, for a given power, the currents increase.) One of the largest standard waveguide sizes, WR2300, with a width of 23 inches (58.4 cm), has a low-frequency cutoff of 257 MHz. One of the smallest, WR3, with a width of 0.03 inches (0.076 cm), has a low-frequency cutoff of 197 GHz.

For a standard (width = 2 × height) waveguide, the fundamental mode, called the *TE_{10} mode*, is the only possible mode for frequencies above the low-frequency cutoff and below twice the low-frequency cutoff. Other modes exist above this one-octave range. At frequencies where higher modes are possible, these modes can be unintentionally excited at sharp bends, robbing power from the desired mode. This power does not couple properly to circuit elements designed for the fundamental mode and dissipates in the walls. Whenever possible, a microwave system designer therefore tries to use only the fundamental mode.

The essential details of this most important mode are derived and discussed below.

16.2 Exact solution: a plane wave interference pattern matches the waveguide boundary conditions

Exact solutions for the E and B fields within waveguides of arbitrary shape are normally deduced through a head-on assault using Maxwell's equations.

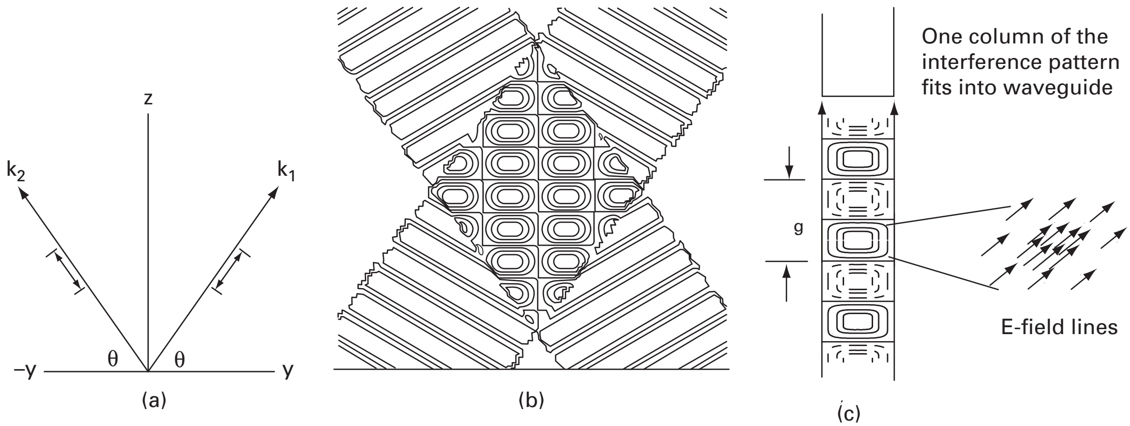

Figure 16.2. Superposition of two plane waves (a) produces an interference pattern (b) streaming in the *z*-direction. One (or more) columns of that pattern satisfies waveguide boundary conditions (c). *E* is in the *x*-direction (coming out of the page).

However, for rectangular waveguides, an exact solution can be obtained indirectly by setting up two plane waves in empty space.

A single plane wave satisfies Maxwell's equations inside a waveguide, but cannot satisfy the boundary conditions at the metal walls. However, the superposition of two properly chosen plane waves forms a traveling interference pattern which does satisfy the boundary conditions and is therefore a valid solution to the waveguide problem. This solution technique can be compared with the "image charge" method in electrostatics, often introduced as a technique to solve for the electric field when a point charge sits alone above an infinite metal sheet. An equal but opposite charge is placed at the mirror image point behind the sheet and the sheet is removed. The electric field lines connecting the charges pass perpendicularly through the x–y plane, satisfying the boundary condition that the E field must be perpendicular when intersecting a conducting surface. The superposition of the two fields, that of the actual charge and that of the image charge, is the solution to the original problem.

Here we construct a solution by superposing two plane waves, identical except for their propagation directions. Both plane waves will be polarized in the x-direction, i.e., their electric fields are in the x-direction. Since electromagnetic waves in free space are transverse waves, the propagation vectors, $\boldsymbol{k}_1$ and $\boldsymbol{k}_2$,[2] corresponding to these waves must both lie in the y–z plane, as shown in Figure 16.2(a).

The first wave, with propagation vector $\boldsymbol{k}_1$, travels in the NNE direction, while the other, $\boldsymbol{k}_2$, travels NNW. In (b), the plane waves are drawn as streams with finite width. Contour lines of the electric field are perpendicular to the directions of propagation. Figure 16.2(b) shows that, in the area where the streams overlap, the sum of the individual electric fields produces an *interference pattern* consisting of columns of cells which stream northward in the z-direction. If we could watch two waves come together in the ocean, we

[2] By definition, the propagation vector, $\boldsymbol{k}$, is in the direction of travel, i.e., perpendicular to the wavefront, and has magnitude $|\boldsymbol{k}| = 2\pi/\lambda$.

would see them produce this interference pattern. As the streams leave the overlap region, they recover their original plane wave form. In the interference pattern, the contour lines of constant E resemble squared-off ovals. (Remember that $\boldsymbol{E}$ is always perpendicular to the page; the oval-like figures are contours of field strength; they are not field lines.)

The pattern formed by a column of cells (Figure 16.2c) solves the waveguide problem if the width of the cells is equal to a, the width of the waveguide. Why is this a solution? First, the electric field at the side walls is zero at all times, satisfying the boundary condition that, at a conducting wall, there can no parallel electric field. Second, the electric field is always in the x-direction, so it is perpendicular where it intersects the top and bottom walls, satisfying the boundary on those walls as well. Third, each plane wave and therefore their sum, is a solution to Maxwell's equations in empty space, i.e., the interior of the waveguide. What about all the columns of cells outside the boundary of the waveguide? We can forget them, just as we ignore the electric field on the image charge side of the x–y plane in the electrostatic example.

Let us apply a little algebra to find the wave's propagation vector, cutoff frequency and phase velocity. Let k denote the magnitude of $\boldsymbol{k}_1$ and $\boldsymbol{k}_2$ so that $\boldsymbol{k}_1 = k\cos(\theta)\,\hat{\boldsymbol{y}} + k\sin(\theta)\,\hat{\boldsymbol{z}}$ and $\boldsymbol{k}_2 = -k\cos(\theta)\,\hat{\boldsymbol{y}} + k\sin(\theta)\,\hat{\boldsymbol{z}}$. The electric field is the sum of the fields of the two waves, i.e.,

$$E(r,t) = \frac{-E}{2\mathrm{j}}\mathrm{e}^{\mathrm{j}(\omega t - k_1\cdot r)} + \frac{E}{2\mathrm{j}}\mathrm{e}^{\mathrm{j}(\omega t - k_2\cdot r)}, \tag{16.1}$$

where the vector $\boldsymbol{r}$ denotes position in the y–z plane and E is a constant equal to the twice maximum electric field of each wave. The amplitudes, $-E/(2\mathrm{j})$ and $E/(2\mathrm{j})$, have been chosen so that $y=0$ will be a column boundary and also to phase the E field to be maximum at $z=0$ when $t=0$. Substituting the expressions for $\boldsymbol{k}_1$ and $\boldsymbol{k}_2$, we have

$$\begin{aligned} E &= E\left(-\mathrm{e}^{(\mathrm{j}\omega t - k(z\cos\theta + y\sin\theta))} + \mathrm{e}^{\mathrm{j}(\omega t - k(z\cos\theta - y\sin\theta))}\right)/(2\mathrm{j}) \\ &= E\sin(ky\sin\theta)\mathrm{e}^{\mathrm{j}(\omega t - kz\cos\theta)}. \end{aligned} \tag{16.2}$$

As always, it is the real part of $\boldsymbol{E}$ that is the actual electric field. Note that all the y dependence is contained in the expression $\sin(k\sin(\theta)\,y)$. This is independent of t, so, in the y-direction, the diffraction pattern is a standing wave. The z and t dependence, however, are contained in the wave factor $\mathrm{e}^{\mathrm{j}(\omega t - kz\cos\theta)}$, so the entire diffraction pattern propagates in the $(+z)$-direction with an effective wavevector $k_{\text{guide}} = k\cos\theta$. For a wave of a given frequency, we can find the value of θ that satisfies the side-wall boundary condition. Suppose that the bottom wall of the waveguide extends from $y=0$ to $y=a$, i.e., the guide width is a. The boundary condition at $y=0$ is satisfied for any value of θ, since $\sin(0)=0$. But the boundary condition at $y=a$ demands that $\sin(k\sin(\theta)\,a)=0$. This will be satisfied if $k\sin(\theta)\,a = n\pi$, where n is an integer. Here we will let $n=1$, so that $\sin(\theta) = \pi/(ka)$ and $\cos(\theta) = (1-[\pi/(ka)]^2)^{1/2}$. Thus the E field in the waveguide is

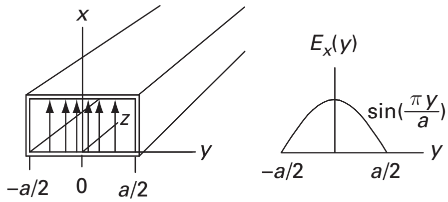

Figure 16.3. Electric field configuration in the TE_{10} mode.

given by (the real part of) $E = E\sin(\pi y/a)e^{j(\omega t - k_g z))}$ where $= k\cos(\theta) = k(1-[\pi/(ka)]^2)^{1/2}$. Figure 16.3 shows how the magnitude of the E field is a maximum at the center line of the waveguide and falls to zero at the side walls.

16.2.1 Guide wavelength

From the expression for k_g, we see that the spatial period along the waveguide will be $2\pi/k_g$. Solving for this length, known as the *guide wavelength*, we find

$$\lambda_{\text{guide}} = \frac{\lambda}{\sqrt{1-\left(\frac{\lambda}{2a}\right)^2}.} \tag{16.3}$$

16.2.2 Magnetic field

Just as the electric field in the guide is the superposition of the electric fields of two plane waves, the magnetic field is the superposition of their magnetic fields. For a plane wave, the magnetic field is perpendicular to both the electric field and the propagation vector,

$$\boldsymbol{B} = \hat{k} \times \mathbf{E}/c, \tag{16.4}$$

where c is the speed of light. The magnetic fields of our two plane waves have z-components as well as y-components, so the magnetic field in the waveguide is not purely transverse with respect to the direction of propagation. In this TE_{10} mode and all other TE modes, only the electric field is purely transverse. There are also TM modes, in which only the magnetic field is purely transverse. Waveguides, unlike coaxial cable, have no TEM modes, in which both E and H fields are transverse.

We can use Equation (16.4) to find the magnetic of field each plane wave and then sum them to get the field in the waveguide. The result is

$$\frac{B_y}{E} = \frac{k_g}{\omega}\sin\left(\frac{\pi y}{a}\right)e^{j(\omega t - k_g z)} \tag{16.5}$$

and

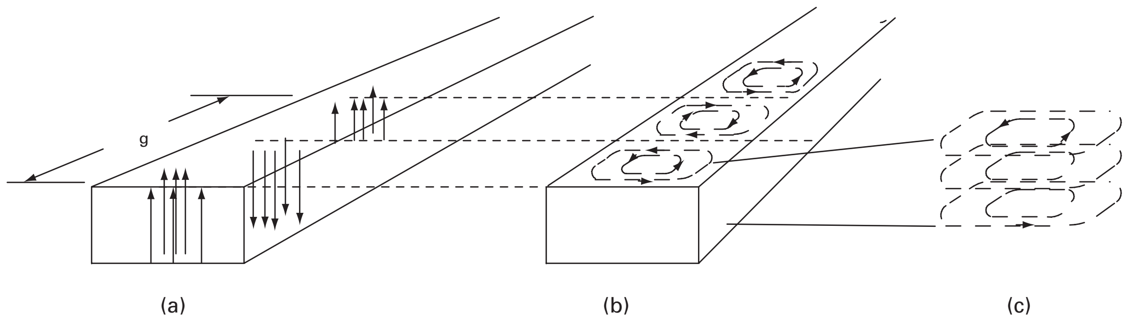

Figure 16.4. Electric field lines (a) and magnetic field Lines (b) The electric lines are bundles of vertical vectors while the magnetic lines are stacks of concentric loops (c.).

$$\frac{B_z}{E} = \frac{\pi}{\mathrm{j}a\omega}\cos\left(\frac{\pi y}{a}\right)\mathrm{e}^{\mathrm{j}(\omega t - k - gz)}. \tag{16.6}$$

The form of this B field is shown in Figure 16.4(b).[3]

Note that the magnetic field lines are stacked concentric loops in the y-z plane with no component normal to the walls. You can use Equations (16.5) and (16.6) to find the exact shape of these loops (see Problem 16.4).

16.2.3 Wall currents

Wall currents, which flow on the inside surfaces of the waveguide, are determined by the tangential magnetic field. The currents are perpendicular to the B field and their magnitude (in amperes/meter) is given by B/μ_0 (the permeability of free space, μ_0, is equal to $4\pi{\cdot}10^{-7}$). The wall currents are indicated in Figure 16.5. These currents converge or diverge from areas on the broad wall

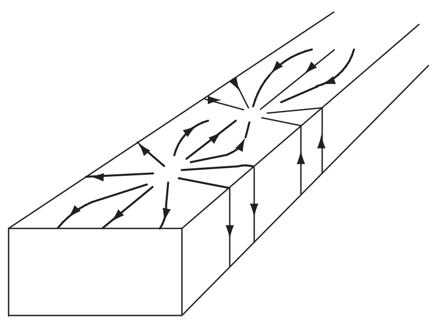

Figure 16.5. Wall currents (solid lines) in relation to the magnetic field (dashed lines).

[3] The reader familiar with Maxwell's equations can quickly derive Equations (16.5) and (16.6) from Equation (16.2) by applying the curl E equation, which here becomes $\mathrm{j}\omega B_y = -\partial E_x/\partial z$ and $\mathrm{j}\omega B_x = \partial E_x/\partial y$.

where positive charge is arriving or leaving. The E-field lines start and end at these charge patches. Note that the currents on the narrow walls are perfectly vertical because the tangential magnetic field has no x-component.

The fields and currents shown in Figures 16.2–16.5 are, of course, snapshots at an instant in time. As the wave propagates, these patterns move uniformly along the z-axis with a (phase) velocity given by $v_{ph} = \omega/\beta$.

16.3 Waveguide vs. coax for low-loss power transmission

Consider a situation requiring a low-loss transmission line. Let us compare a standard 2:1 aspect ratio waveguide to a cylindrical coaxial line. To minimize the loss we will make both as large as possible, but here we will impose the restriction that they are also small enough so that modes higher than the fundamental mode cannot propagate. Appendix 16.1 shows that the diameter of this lowest-loss coaxial line and the height of the lowest-loss waveguide are very close to $\lambda/2$ and that the coaxial line will have 2.4 times the loss of the waveguide and will carry only 23% as much power before breakdown.

16.4 Waveguide impedance

There are several ways to define an impedance for a waveguide. One way is to define the voltage to be the potential difference between the top and bottom walls at the middle of the guide and the current to be the integrated current across the top wall. The ratio of voltage to current gives an impedance. Another definition uses voltage and power flow. Still another method uses the ratio of electric field to magnetic field at the center of the guide. The various definitions give $Z_0 = 377$ ohms (impedance of free space) within a factor of 2. But regardless of how impedance is defined, there is no ambiguity in the concept of reflection coefficient. Recall that a shunt capacitance on an ordinary (TEM) transmission line produces a reflection coefficient on the negative j-axis of the Smith chart. The same kind of reflection is produced in a waveguide by a short vertical post or a horizontal iris. These obstructions are therefore called "capacitive posts" or "capacitive irises." An iris across the narrow dimension of the guide causes a reflection on the positive j-axis so is called an "inductive iris." Figure 16.6 shows examples of inductive and capacitive irises. (The equivalent circuit for a thin iris is just a single shunt susceptance.)

Figure 16.6. Waveguide irises: (a) inductive iris; (b) capacitive iris.

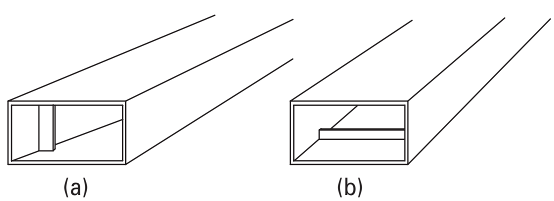

https://doi.org/10.1017/CBO9780511626951.017 Published online by Cambridge University Press

The combination of an inductive and a capacitive iris (a thin wall with a hole) is equivalent to a parallel resonant circuit. You can see how these resonant irises could be spaced at quarter-wave intervals in a waveguide to make a coupled-resonator filter.

16.5 Matching in waveguide circuits

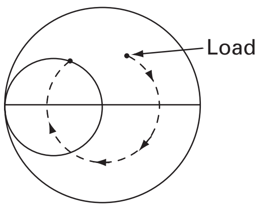

Figure 16.7. A load's reflection coefficient located on the Smith chart.

Impedance matching in waveguide circuits can be done with the same techniques used for ordinary transmission lines. Suppose we are using a waveguide to supply power to some device, maybe a horn antenna, and that we have an instrument – a reflectometer or network analyzer – that can measure the reflection coefficient looking into the waveguide. We can locate the reflection coefficient on the complex reflection plane (Smith chart) as shown in Figure 16.7.

As we move down the guide, away from the load, the reflection coefficient circles the center of the chart and eventually arrives at the unity conductance circle. We locate this position on the guide and install the appropriate inductive or capacitive iris. In practice the tuning process is sometimes very simple: we find the point at which we need to add shunt capacitance. If the reflected wave is small (not a severe mismatch) we do not have to add much capacitance so we get out the ball-peen hammer and dent the broad side of the guide. An expert learns just how hard to swing the hammer.

A note on matching: suppose we join two dissimilar waveguides (perhaps of different sizes) at a junction, which could be some kind of elbow, coupling, butt joint, etc. Assume that the system is nominally lossless, i.e., all metal. We want to match the junction so that a wave coming from either direction will suffer no reflection. We carry out the above procedure on one side of the junction. Do we have to then match the other side? No, the job has been done. Time-reversal produces an equally good solution to Maxwell's equations in which all the power flows in the opposite direction. Of course this applies just as well to ordinary (TEM) transmission lines as it does to waveguides. This simple argument fails for lossy junctions because the time-reversed solution requires the absorptive material to *produce* power, but a stronger argument, based on the reciprocity theorem leads to the same conclusion.

16.6 Three-port waveguide junctions

Two kinds of waveguide T-junctions (three-port junctions) are shown in Figure 16.8.

The *series-T* gets its name from the fact that the voltage of the input guide divides between the two output guides. This works out well because the half-height output guides have half the impedance of the input guide and the junction is inherently matched. (The half-height guides could be increased to full-width in a gradual taper that would not cause much reflection.) The *shunt-T* applies the full input voltage across each of the output arms – not such a natural as the series-T.

https://doi.org/10.1017/CBO9780511626951.017 Published online by Cambridge University Press

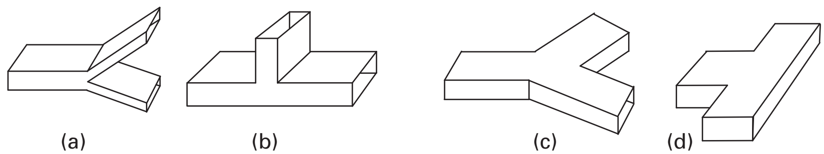

Figure 16.8. Waveguide T-junctions.

16.7 Four-port waveguide junctions

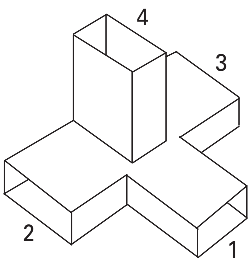

Figure 16.9. Waveguide Magic T.

The *Magic T* hybrid can be built using a procedure that itself seems like magic. We start with the bare waveguide junction (nothing hidden inside) as shown in Figure 16.9.

First we match Port 1, i.e., eliminate reflections from Port 2 when the other ports are feeding matched, i.e., reflectionless, loads. To do this we start by putting matched loads on Ports 2 and 3. (We do not have to put a load on Port 4 since, by symmetry, it is isolated from Port 1.[4]) With the loads in place we measure the reflection at Port 1 and install the necessary iris (or dent) somewhere down line 1. Then we do the same process on Port 4. That's it. The two matches and the isolation by virtue of symmetry are sufficient. We now have a perfectly matched Magic T hybrid.

Simple narrowband transitions from coax to waveguide have mostly been built with empirical methods. With the aid of three-dimensional finite element simulation programs, wideband transitions have been designed. In general, the designer first looks at the fields on both sides and finds a mechanical structure that causes the main features of the fields to line up. The remaining reflection should be small and can be tuned out with a small iris or other structure whose complexity depends on the desired bandwidth.

Rectangular waveguides, like TEM lines, can carry only one signal in each direction. But square or round guides can have two independent waves; they are both fundamental mode waves but they have different polarizations. To launch or recover these two waves independently requires an *orthomode coupler*, which has no TEM counterpart. The simplest orthomode couplers use coaxial or waveguide connections mounted at right angles on the sides of the square or round guide. Some couplers produce circular rather than rectangular polarizations. Wideband orthomode transitions are always needed for radio astronomy and their development is an active field.

[4] The E field is vertical as a wave enters Port 1. Would it point left or right as it emerged from Port 4? Since the geometry is symmetric, there is no reason to favor right or left. Hence, no wave emerges from Port 4.

Appendix 16.1 Lowest loss waveguide vs. lowest loss coaxial line

For lowest loss we will make the waveguide and the coaxial line as large as possible, but, as explained above, with the restriction that each be capable of supporting only its fundamental mode. Our lowest loss $TE_{1,0}$ waveguide will be made with its width equal to the wavelength. (If it is any wider, the second mode, $TE_{2,0}$, becomes possible.) We will make the height equal to half the width, i.e., the usual aspect ratio. For air-filled coaxial line at the frequency where non-TEM modes become possible, the inner and outer radii, r_i and r_o, satisfy the inequality $(r_o + r_i)\,\pi \geqq 1.03\lambda$.[5] The equal sign applies when $r_i / r_o = 1/3.6$. This ratio also provides the lowest loss air-filled coaxial line for a given outer diameter (see Appendix 16.2). Note that the characteristic impedance, $Z_0 = 60\ \ln\,(r_o / r_i)$, will be 77 ohms for this lowest-loss coaxial cable. Using this ratio of diameters, the maximum outer diameter is given by $r_o = 1.03\lambda\pi^{-1}/(1{+}1/3.6) = 0.26\lambda$. These relative waveguide and coax cross-sections are shown in Figure 16.10.

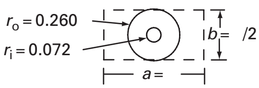

Figure 16.10. Relative cross-sections of lowest-loss waveguide and coaxial cable.

Let us compare the losses. The amplitude of a wave propagating in the $(+x)$-direction on any lossy line is proportional to $\exp(-\alpha x)$ where α, the loss factor, has units of inverse meters. The power is therefore proportional to $\exp(-2\alpha x)$ and the fractional power loss per meter is 2α. Note that $20\log(e)\alpha = 8.686\alpha$ dB/meter. Because of the skin effect, the loss of a line is proportional to its surface resistance which is given by

$$R_S = \sqrt{\frac{\omega\mu}{2\sigma}} \quad \text{ohms per square} \tag{16.7}$$

where σ is the bulk dc conductivity and ω is the (angular) frequency. (For copper, $R_s = 2.61 \times 10^{-7}$ ohms/$\sqrt{\text{Hz}}$; for aluminum, $R_s = 3.26 \times 10^{-7}$ ohms/$\sqrt{\text{Hz}}$). The loss factor for air-filled coax line is given by

$$\alpha_{\text{coax}} = \frac{R_s}{2Z_0}\left(\frac{1}{2\pi r_o} + \frac{1}{2\pi r_i}\right). \tag{16.8}$$

Our lowest loss coax line has $Z_o = 77$, $r_o = 0.26\lambda$ and $r_i = 0.072\lambda$ so its loss becomes

$$(\alpha_{\text{coax}})_{\min} = 0.0183\,\frac{R_s}{\lambda}. \tag{16.9}$$

For air-filled rectangular waveguide in the fundamental mode the loss factor is given by

$$\alpha_{WG} = \frac{R_s}{377}\,\frac{\left(1 + \dfrac{2b}{a}\left(\dfrac{\lambda}{2a}\right)^2\right)}{b\sqrt{1 - \left(\dfrac{\lambda}{2a}\right)^2}} \tag{16.10}$$

[5] Reference [2], p. 42.

where 377 ohms is $\sqrt{\mu_0/\epsilon_0}$, the "impedance of free space." In our case $a = 2b = \lambda$ so

$$(\alpha_{\mathrm{WG}})_{\min} = \frac{R_s}{\lambda}\frac{5}{337\sqrt{3}} = 0.0076\frac{R_s}{\lambda}. \tag{16.11}$$

The loss of the coax is therefore higher than that of the waveguide by a factor of 0.0183/0.0076 or about 2.4. What about power handling capacity? The breakdown of either the waveguide or the coax depends on the maximum E field, $E_{\max}$. (For air at sea-level pressure, $E_{\max}$ is about 30 000 volts/cm.) For rectangular waveguide in the fundamental mode the power is related to the maximum E field by

$$\frac{\mathrm{Pwr}}{{E_{\max}}^2} = \frac{1}{4\cdot 377}ab\frac{\lambda_0}{\lambda_g} = 6.63 \times 10^{-4}ab\frac{\lambda_0}{\lambda_g} \tag{16.12}$$

where Pwr is in watts, $E_{\max}$ is in volts/cm, a and b are in cm, λ_0 is the free-space wavelength, and λ_g, the guide wavelength, is given by

$$\lambda_g = \frac{\lambda_0}{\sqrt{\left(1 - \left(\frac{\lambda_0}{\lambda_{\mathrm{cutoff}}}\right)^2\right)}}. \tag{16.13}$$

For our waveguide $\lambda_0/\lambda_{\mathrm{cutoff}} = 1/2$ so $\lambda_g = 2\lambda_0/\sqrt{3}$ and

$$\frac{\mathrm{Pwr}}{{E_{\max}}^2} = 5.74 \times 10^{-4}ab = 5.74 \times 10^{-4}\lambda\,\lambda/2 = 2.37 \times 10^{-4}\lambda^2. \tag{16.14}$$

Turning to the coax, the ln(r) dependence of voltage and the characteristic impedance, $Z_0 = (377/2\pi)\ln(r_o/r_i) = 60\ln(r_o/r_i)$ allow us to find the power in terms of the maximum E field:

$$\frac{\mathrm{Pwr}}{{E_{\max}}^2} = \frac{Z_0 r_i^2}{2\cdot 60^2}. \tag{16.15}$$

In our case $Z_0 = 77$ and $r_i = 0.072\lambda$ so

$$\frac{\mathrm{Pwr}}{{E_{\max}}^2} = \frac{77}{2\cdot 60^2}(0.072\lambda)^2 = 0.55 \times 10^{-4}\lambda^2. \tag{16.16}$$

We see that the waveguide can handle 2.37/0.55 = 4.3 times the power of the minimum loss coaxial line. The waveguide is clearly better both for loss and power handling capacity. In high-power applications the waveguide has the additional advantage that there are no interior surfaces needing cooling and no mechanical spacers to center an inner conductor. (Insulating spacers in high-power coaxial lines must fit tightly; high voltage develops across any gap. This problem generally reduces the power-handling capacity of the coaxial line by something like an order of magnitude.)

Appendix 16.2 Coax dimensions for lowest loss, highest power, and highest voltage

Lowest loss

For a given outer diameter, the characteristic impedance of a coaxial line is increased by making the inner diameter smaller. For a given power, the current is decreased. But the smaller inner conductor has more resistance. The I^2R product, i.e., the dissipation, has a minimum when the ratio of diameters is 3.6. This follows from Equation (16.8) which can be rewritten as

$$\alpha_{\text{coax}} = \frac{R_s}{2 \cdot 60 \cdot 2\pi r_o} \frac{1}{\ln(x)} (1 + x) \tag{16.17}$$

where $x = r_o/r_i$. The minimum of $(1+x)/\ln(x)$ occurs at $x = 3.6$ so the characteristic impedance of lowest-loss air-filled coaxial line is $Z_0 = 60 \ln(3.6) = 77$ ohms.

Highest power

From Equation (16.15) we see that to maximize the power-handling capability of the coaxial line we must maximize the expression $Z_0\, r_i^2$, i.e., we must maximize $\ln(x)/x^2$. The maximum occurs when $\ln(x) = 1/2$ so the characteristic impedance of the maximum power line is $Z_0 = 60/2 = 30$ ohms.

Maximum voltage

If the line is to withstand maximum voltage the optimum value of $\ln(x)$ is 1 and the characteristic impedance is 60 ohms. This also follows from Equation (16.15): if we express power as $V_{\max}{}^2/(2Z_0)$ then $V_{\max}$ is proportional to $Z_0\, r_i$ or $\ln(x)/x$, which reaches a maximum at $x = e$.

Relative performance of 50-ohm coaxial line

The 50-ohm line commonly used in RF work ($x = r_o/r_i = 2.3$) strikes a compromise between lowest loss, highest power and highest voltage. For loss, we compare $(1+x)/\ln(x)$ for $x = 2.3$ and $x = 3.6$ to see that the 50-ohm line will have only 10% more loss than a 77-ohm line with the same outer diameter. For power handling, we compare $\ln(x)/x^2$ and find that the 50-ohm line can carry 62% as much power as a 30-ohm line with the same outer diameter. Finally, for voltage we compare $\ln(x)/x$ and find that the 50-ohm line can handle 98% as much voltage as a 60-ohm cable with the same outer diameter.

Problems

Problem 16.1. Suppose a car enters a long tunnel which is essentially a rectangular metal tube 10 meters wide by 5 meters high. The car radio becomes silent inside the tunnel. Was the radio more likely tuned to an AM station or an FM station?

Problem 16.2. Examine the waveguide current distribution shown in Figure 16.5 (for the fundamental mode) and draw a sketch showing the position(s) in which a narrow slot could be cut through the waveguide wall without affecting its operation.

Problem 16.3. Describe an experimental setup that could be used to demonstrate the waveguide E-field and B-field distributions shown in Figure 16.4.

Problem 16.4. In the discussion just above Equation (16.2), let $n = 2$ instead of 1. For this choice of n (the TE_{20} mode), find the cutoff wavelength and the guide wavelength. Sketch the electric and magnetic field lines.

Problem 16.5. Use Equations (16.5) and (16.6) to find the mathematical shape of the magnetic field loops. Hint: the slope of a field line, dz/dy, is given by B_z/B_y. Set up the equation $dz/B_z = dy/B_y$ and note that the left side contains only z while the right side contains only y. They can therefore be integrated separately. Remember to add a constant of integration.

References

[1] Collin, R. E., *Foundations for Microwave Engineering*, New York: McGraw Hill, 1992.

[2] Montgomery, C. G., Dicke, R. H. and Purcell, E. M., *Principles of Microwave Circuits*, London: Peter Peregrinus, 1987 (originally Volume 8 of the MIT Radiation Laboratory Series, New York: McGraw Hill, 1948).

[3] Moreno, T., *Microwave Transmission Design Data*, Sperry Gyroscope Corp, 1948, reprinted by Dover Publications, 1958.

[4] Ramo, S., Whinnery, S. R. and Van Duzer, T. *Fields and Waves in Communication Electronics*, 3rd edn., New York: John Wiley, 1994. (Original edition was Ramo, S. and Whinnery, S. R., *Fields and Waves in Modern Radio*, New York: John Wiley, 1944).

https://doi.org/10.1017/CBO9780511626951.017 Published online by Cambridge University Press